Electronic Supplementary Material (ESI) for Nanoscale
This journal is © The Royal Society of Chemistry 2012

Supporting Information

Facile Thermal Treatment Process for Assembling Vertically Aligned Semiconductor Nanorods in Solution

Albert M. Hung, Taeseok Oh, Jennifer N. Cha

1. Synthesis of CdSe nanorods

The procedure for synthesizing CdSe nanorods was adapted from the literature[1] and was the same as previously reported.[2] Briefly, 137 mg of cadmium oxide (CdO, 99.95%, -325 mesh, Alfa Aesar), 595 mg of tetradecylphosphonic acid (TDPA, 97%, Strem Chemicals) and 1.935 g of trioctylphosphine oxide (TOPO, 99%, Aldrich) were loaded into a three-neck flask, heated to 120 °C, and purged with nitrogen for 1 hr. The mixture was then heated at 300 °C until all of the CdO dissolved and the mixture turned clear and colorless, after which it was cooled to room temperature and "aged" overnight. In a glove box, 42 mg of selenium powder (Se, 99.5%, -325 mesh, Alfa Aesar) was dissolved in 127 mg of tributylphosphine (TBP, 97%, Aldrich), 965 mg of trioctylphosphine (TOP, 90%, Aldrich) and 200 mg of toluene (certified ACS, Fisher). The Cd mixture was heated to 120 °C and purged with nitrogen for 1 hr, then heated to 320 °C. The Se solution was injected into the Cd mixture and the temperature was reduced to 250°C for growth. After 20 min of growth, the flask was removed from heat to stop the reaction. Upon cooling, 6 mL of toluene were added to the flask, and the solution was transferred to a centrifuge tube and centrifuged at 5000 RPM (2632 RCF) for 3 min in an Allegra X-22R centrifuge (Beckman-Coulter) to remove any solid matter. The nanorods were rinsed of excess surfactant by precipitating with 3-5 mL of methanol, centrifuging at 3000 RPM (948 RCF) for 3 min, discarding the supernatant, and resuspending the rods in 5 mL of toluene. This step was repeated four more times. Insoluble matter sometimes appeared during washing and was centrifuged out and discarded. Nanorod solutions in toluene were stored at room temperature in vials flushed with nitrogen. To get nanorods in different solvents, an appropriate amount of stock solution was dried under vacuum and resuspended in the desired solvent.

2. Single-crystal nanorod superlattices

Figure S1 shows optical fluorescence and atomic force microscopy (AFM) images of nanorods assembled by thermal treatment of a 1.0 μM nanorod suspension in 28 vol% dioxane/toluene. The assembled platelets were large enough to be observed by optical microscopy with the largest intact platelet measuring almost 24 μM in diameter. The AFM height profile shows that the thickness of the assemblies was close to the length of a single nanorod. Figure S2 shows TEM images and corresponding Fourier transforms (FTs) of a nanorod monolayer assembly obtained by thermal treatment of a 0.2 μM nanorod suspension in 28 vol% dioxane. Platelets up to 10 μm in diameter were observed even at such low nanorod concentrations. The FTs showed little variation in the orientation of the hexagonal lattice at opposite ends of the platelet, and no grain boundaries were observed during TEM imaging (pictures not taken). While tilting of the nanorods obscured some details of their lattice packing,[2,3] this data suggested that the entire 10 μm-wide platelet was a single crystal. It is believed that heat treatment enabled reassembly of the nanorods from a kinetically trapped, disordered state to an ordered state, and the platelets assembled by a nucleation and growth mechanism.

This journal is © The Royal Society of Chemistry 2012

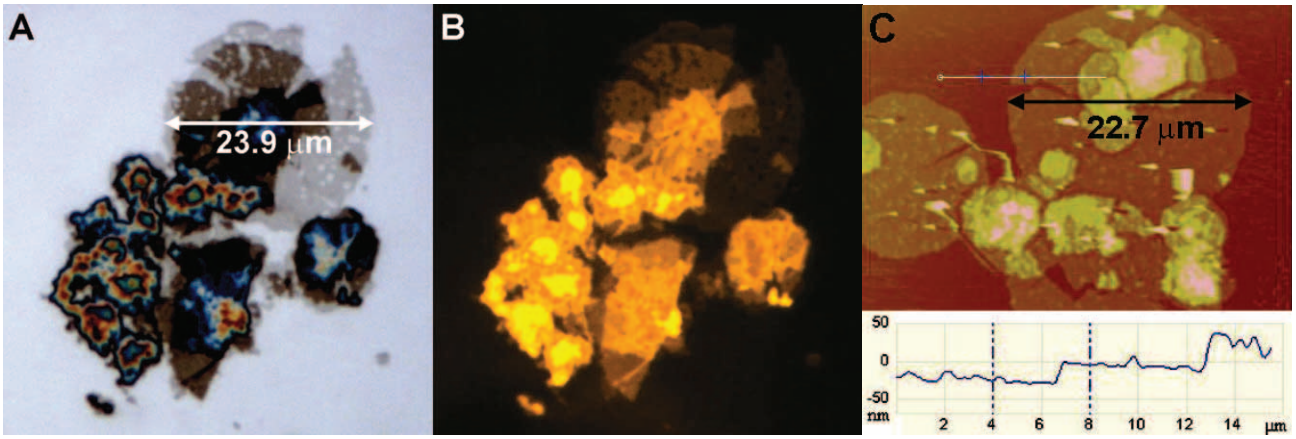

Figure S1. (A) Optical, (B) fluorescence, and (C) AFM images of nanorod assemblies.

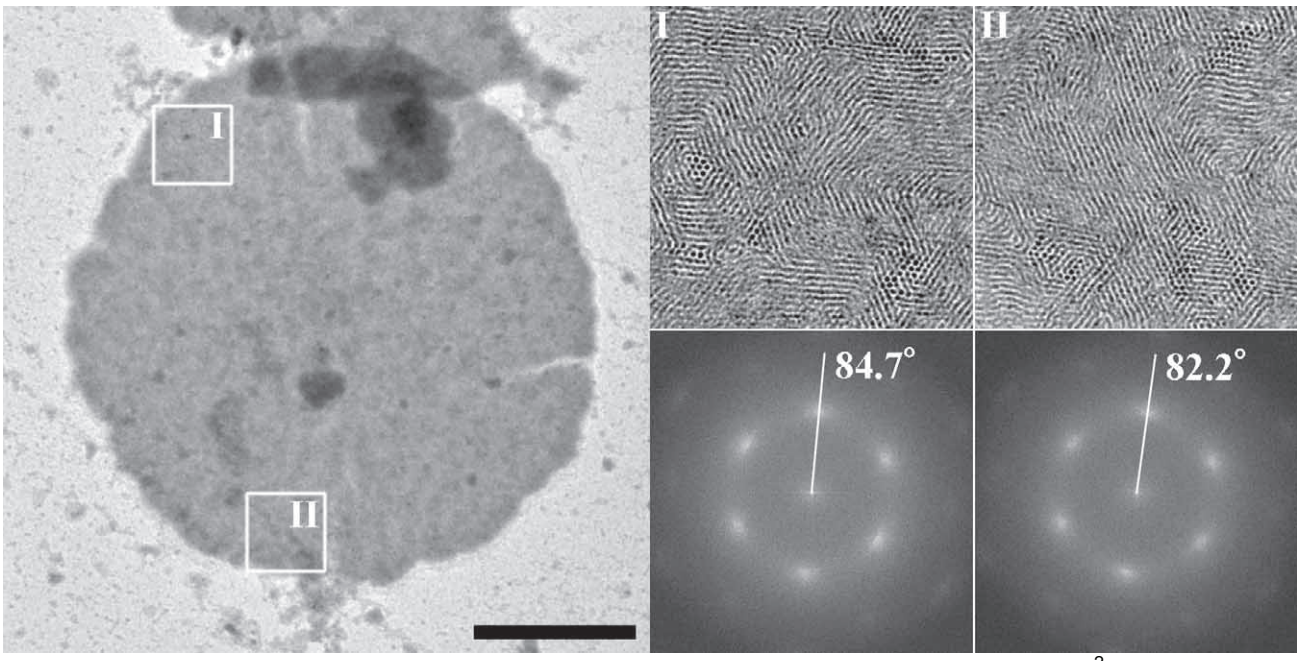

Figure S2. TEM images of a nanorod monolayer assembly. FT analysis of 1 μm^2 areas at opposite ends of the platelet (areas **I** and **II**, 300 nm cropped portions of each image shown on the right) show only slight rotation of the hexagonal superlattice. Scale bar is 3 μm.

3. Vapor-liquid equilibrium of dioxane/toluene mixtures

Table S1 gives Antoine and Wilson parameters for dioxane/toluene mixtures.[4] Assuming ideal gas behavior for the vapor phase, slow evaporation, and no excess volume of mixing, the solvent composition change due to evaporation can be plotted[2] as shown in Figure S3. The isothermal phase diagram shows that the composition of the vapor varies little from the composition of the liquid. While care was taken to avoid solvent evaporation during the thermal annealing experiments, it was safe to say that any evaporation that might have occurred did not change the solvent composition significantly. In the worst-case scenario for example, a loss of 10% of the solution volume due to evaporation might change the solvent composition from 20 vol% dioxane to 19.3 vol% at 20 °C.

This journal is © The Royal Society of Chemistry 2012

Table S1. Vapor-liquid equilibrium data for dioxane/toluene mixtures.[4]

	Molar Volume (mL/mol, 20 °C)	Antoine Constants			Wilson Constants	
		A	B	C	Λ_{12}	Λ_{21}
1,4-Dioxane (1)	85.25	7.43155	1554.68	240.337	0.69200	1.15360
Toluene (2)	106.3	6.95805	1346.77	219.693		

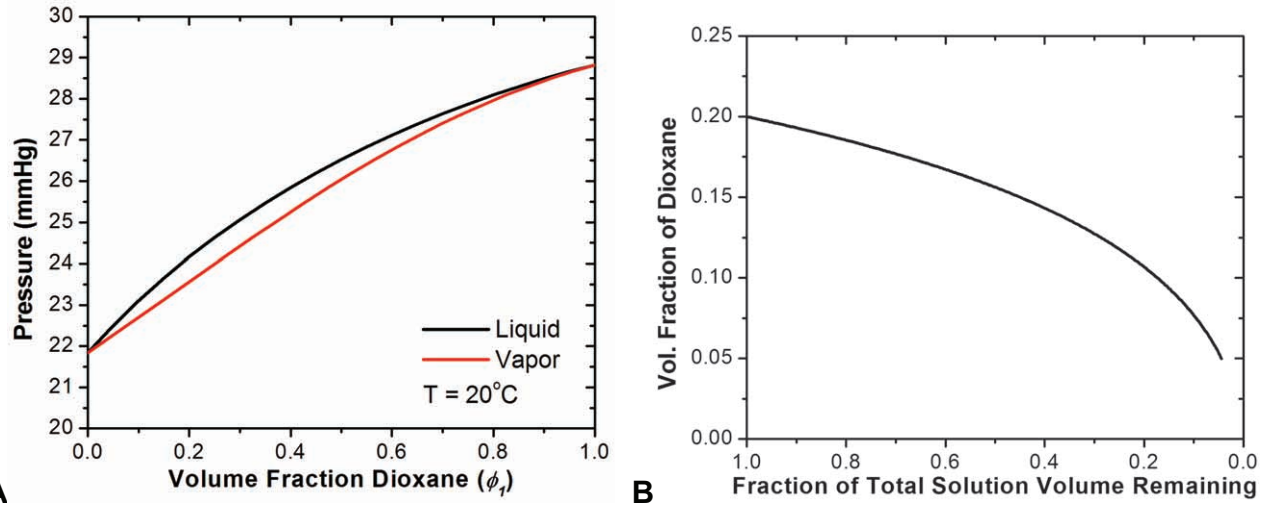

A B

Figure S3. (A) Isothermal vapor-liquid phase diagram for dioxane/toluene mixtures at 20 °C. (B) Example plot of the solvent composition of a dioxane/toluene mixture initially at 20 vol% dioxane as it evaporates at 20 °C. The dioxane evaporates slightly faster, so the concentration of dioxane decreases with evaporation.

4. Effects of solvent composition and nanorod concentration

Polydispersity in nanorod shape and size likely led to some tilting of the nanorods, but solvent selection was a more significant factor. Figure S4 shows TEM images of assemblies drop cast from isopropanol/toluene and isopropanol/choroform mixtures. Because toluene has a lower vapor pressure than isopropanol, the solvent mixture enriched in toluene as it evaporated, leading to slight dissolution of the nanorod assembly. The reverse occurred if "good" solvents with higher vapor pressures (chloroform or hexane) were used instead of toluene, yielding exceptional hexagonal order over the assembled area.

In a solvent mixture of 28 vol% dioxane/toluene, the number averaged width of the assemblies obtained were roughly 5 and 9 μm for nanorod concentrations of 0.2 and 1.0 μM, respectively. Polydispersity in platelet size was very high due to uncontrolled nucleation and fragmentation. Fragmentation ultimately limited the maximum size of the assemblies as shown by the TEM image in Figure S5 of assemblies obtained at a much higher nanorod concentration of 10 μM. The assemblies were large but irregularly shaped (non-circular), suggesting that they were fragments of much larger sheets.

As the concentration of dioxane in solution increased, the number, size, and degree of order of the platelets increased as observed by TEM images shown in Figure S6. Lower concentrations of non-assembled nanorods were also observed at higher vol% dioxane. For dioxane concentrations between 12 and 18 vol%, no ordered assembly was observed at room temperature, but assembly could be achieved if the suspension was cooled to 4 °C (Figures S7 and S8). In all cases, DLS reported an increase in aggregate size and decrease in scattering intensity after thermal annealing.

This journal is © The Royal Society of Chemistry 2012

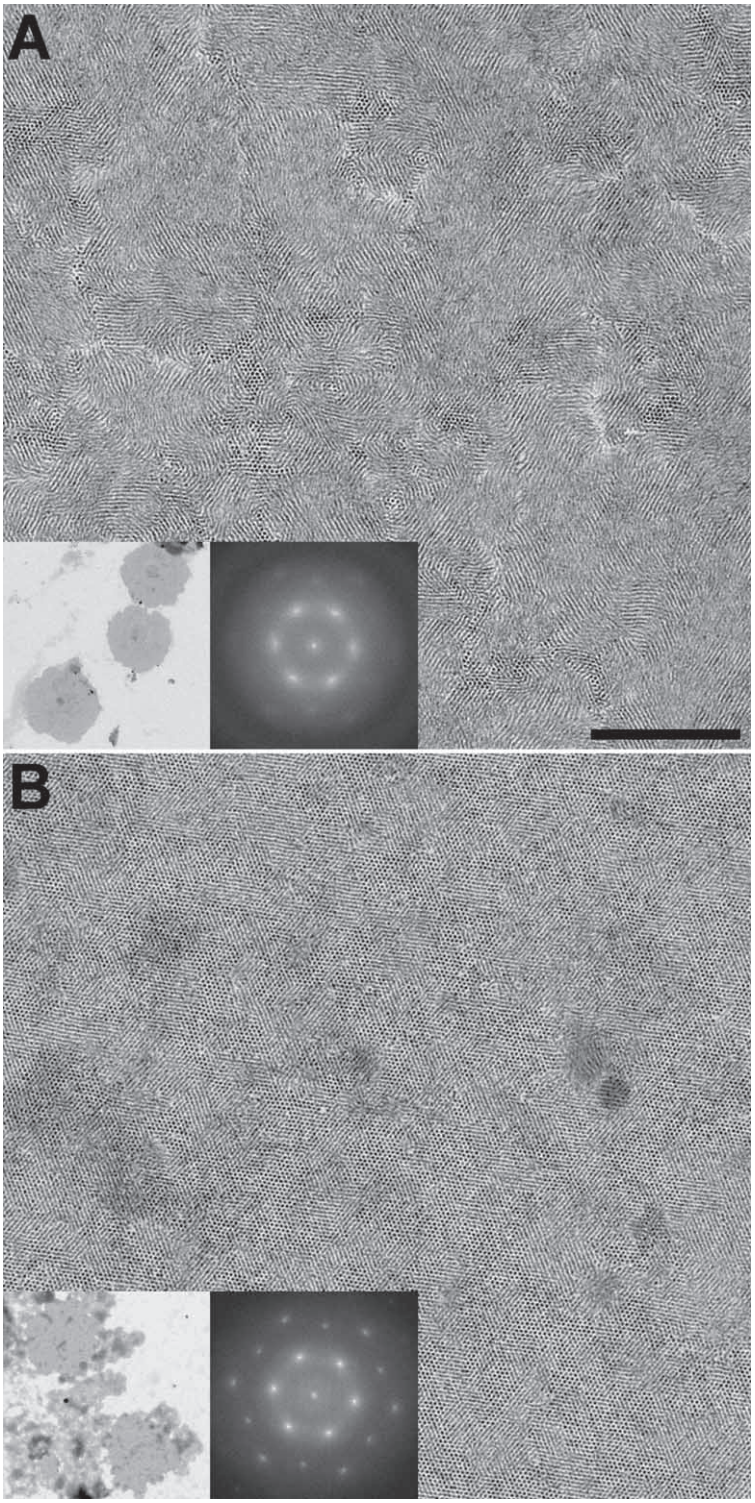

Figure S4. TEM images of 0.2 □M nanorod assembled from (A) 45 vol% isopropanol/toluene and (B) 50 vol% isopropanol/chloroform. Insets are 12 and 5 μm, respectively, and scale bar is 200 nm and applies to both images. Insets also show FTs of the entire 1 μm^2 image area.

This journal is © The Royal Society of Chemistry 2012

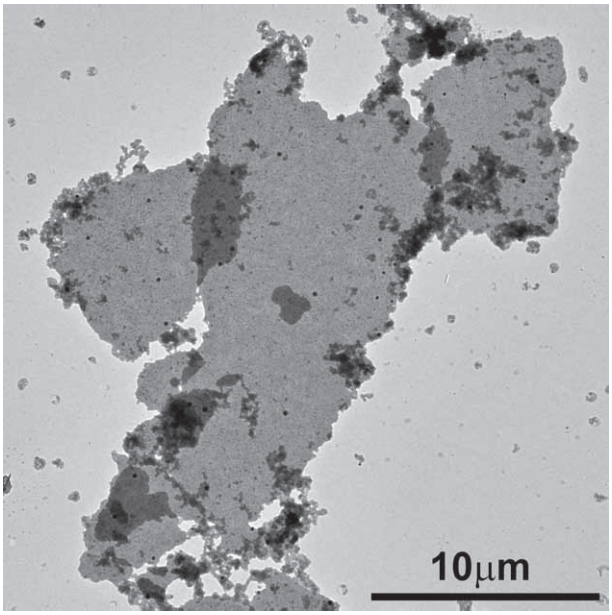

Figure S5. TEM image of assemblies obtained from solutions of 10 μM nanorods in 28 vol% dioxane/toluene.

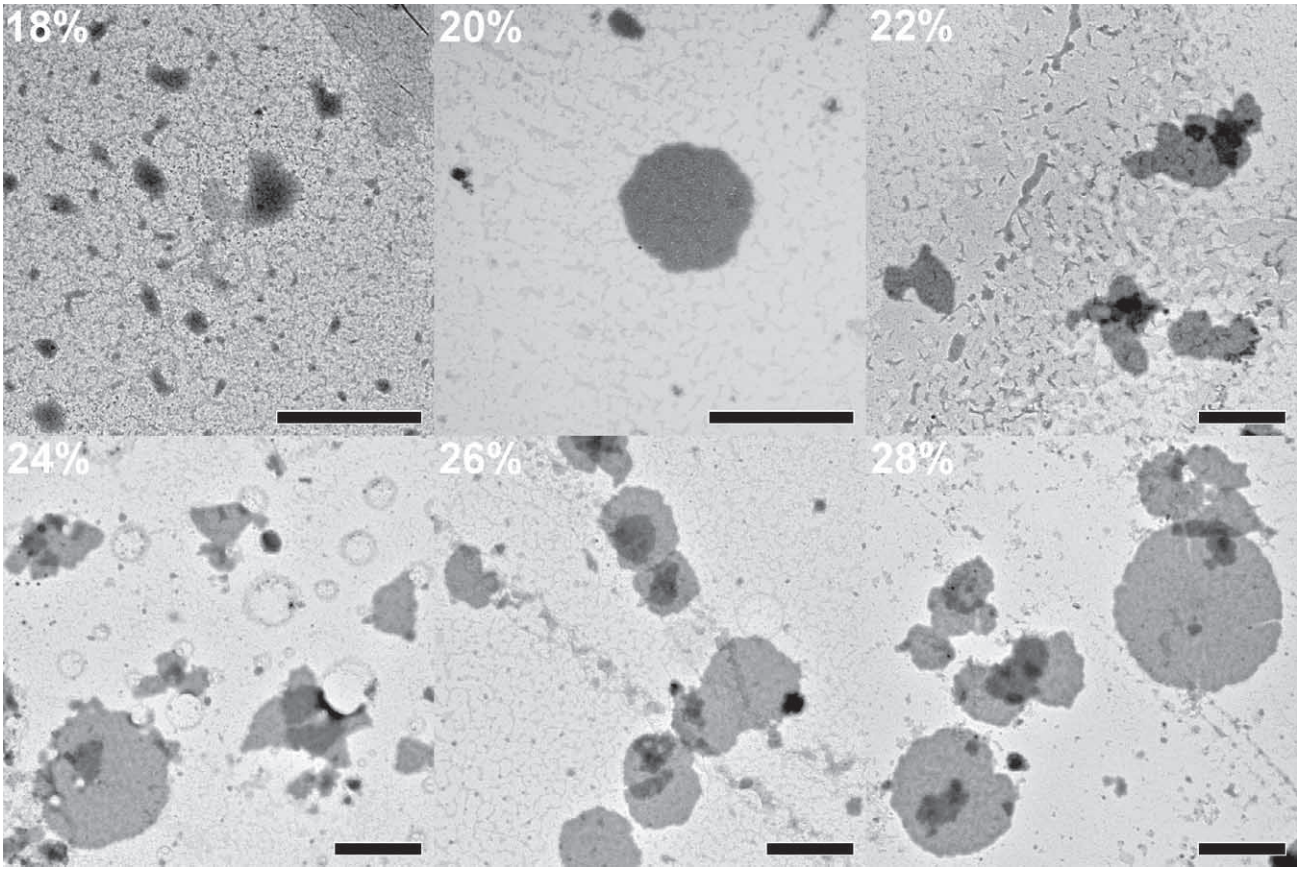

Figure S6. TEM images of 0.2 μM nanorod suspensions at room temperature (21 °C) after thermally assembly in dioxane/toluene mixtures ranging from 18 to 28 vol% dioxane. All scale bars are 5 μm

This journal is © The Royal Society of Chemistry 2012

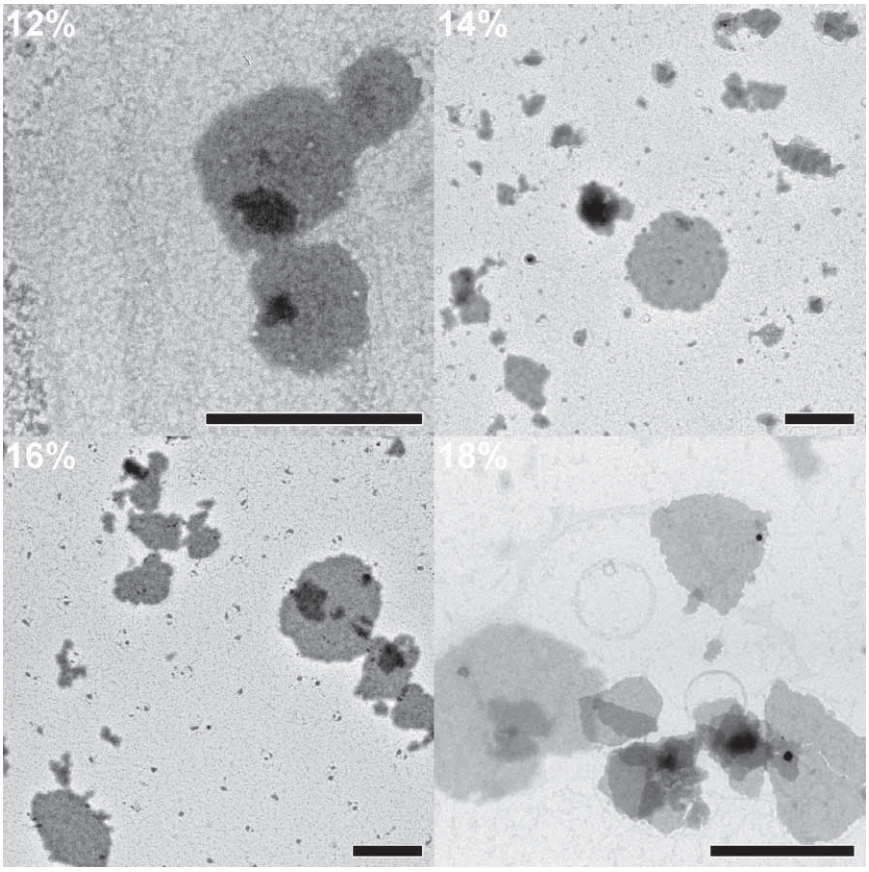

Figure S7. TEM images of 0.2 μM nanorod suspensions at 4 °C after slow cooling from room temperature in dioxane/toluene mixtures ranging from 12 to 18 vol% dioxane. All scale bars are 4 μm

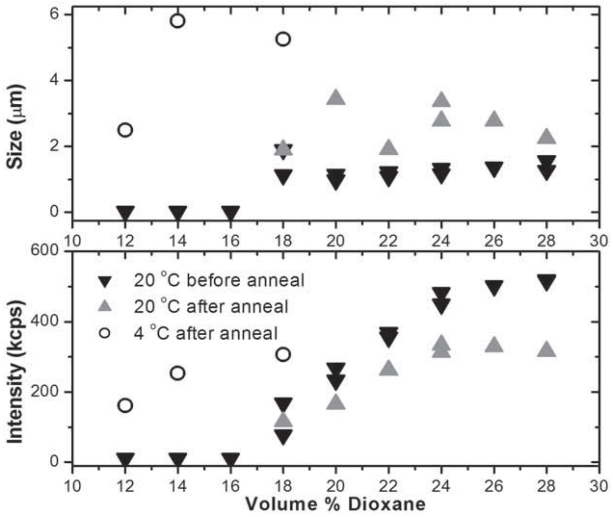

Figure S8. Z-average size and scattering intensity by DLS for 0.2 μM nanorod suspensions in different toluene/dioxane mixtures at 20 °C before and after thermal assembly. For low dioxane concentrations, assembly was achieved by cooling to 4 °C.

This journal is © The Royal Society of Chemistry 2012

5. DLS data of nanorod dispersion and assembly

In order to test how fast aggregation and dissolution of the nanorods could occur, DLS measurements were performed in which the cuvette containing a 0.2 μM suspension of nanorods was transferred immediately from room temperature into the instrument already pre-heated or pre-cooled. The scattering intensity and particle size were measured with time and plotted in Figure S9. Randomly aggregated nanorods in 28 vol% dioxane/toluene melted in under 2 min at 50 °C (Fig. S9a). In comparison, the thermally assembled nanorods took roughly 1 min longer to melt, likely due to their larger size and more close-packed structure. Further investigation of nanorod dissolution nearer to the melting transition showed that the scattering intensity and size still leveled off within 10 min (Fig. S9b). This data helped to confirm the reliability of DLS data taken at heating and cooling rates of 0.1 °C/min.

When nanorods in 16 and 14 vol% dioxane were transferred from room temperature to 4 °C, the scattering intensity jumped sharply, indicating rapid initial aggregation (Fig. S9c). In time, the scattering intensity leveled off but the reported Z-average size continued to grow more slowly, suggesting subsequent diffusion limited aggregation of nanorod clusters. While the aggregation curves for nanorods in 14 and 16 vol% dioxane looked very similar to each other, the curves for 12 vol% showed significantly slower aggregation behavior due to a reduced driving force for assembly. The rate of change of the average hydrodynamic radius r_h near time t = 0 as given by the slopes of the curves in Fig. S9c may be related to the effective association constant K for dimerization. For a suspension of N spherical particles, this relation was expressed as[5,6]

$$\frac{1}{r_{h,1}}\frac{dr_h(t)}{dt}=\frac{I_2(q)}{2\,I_1(q)}\left(1-\frac{r_{h,1}}{r_{h,2}}\right)NK \qquad (1)$$

where I_i is the wave vector (q)-dependent intensity of the scattered radiation and $r_{h,i}$ is the hydrodynamic radius of the monomer (1) or dimer (2). Adapting a similar model for nanorods may allow for the experimental determination of thermodynamic quantities associated with nanorod assembly.

6. Effects of temperature ramp rates

DLS data were typically collected at intervals of 0.5 °C with 2 min equilibration time between each step, translating to an average heating and cooling rate of 0.1 °C/min. At a slightly faster ramp rate of 0.3 °C/min (1.0 °C step size with 1 min equilibration time between each step, Figure S10), the hysteresis was exaggerated only slightly. More severe distortion of the curve was observed for ramp rates of 0.5 °C/min.

The effects of faster cooling rates were investigated by annealing aliquots of 1.0 μM nanorod suspensions in 28 vol% dioxane in a PCR machine and imaging the samples by TEM (Figure S11). In general, the platelet assemblies decreased in both size and hexagonal order with faster cooling rates. However, 3-4 μM wide platelets were still obtained at a cooling rate of 5 °C/min, and decent hexagonal packing was observed at rates as fast as 20 °C/min (2.25 min to cool from 60 to 15 °C). These results suggest that the thermal treatment may not need to be limited to excessively slow cooling rates.

This journal is © The Royal Society of Chemistry 2012

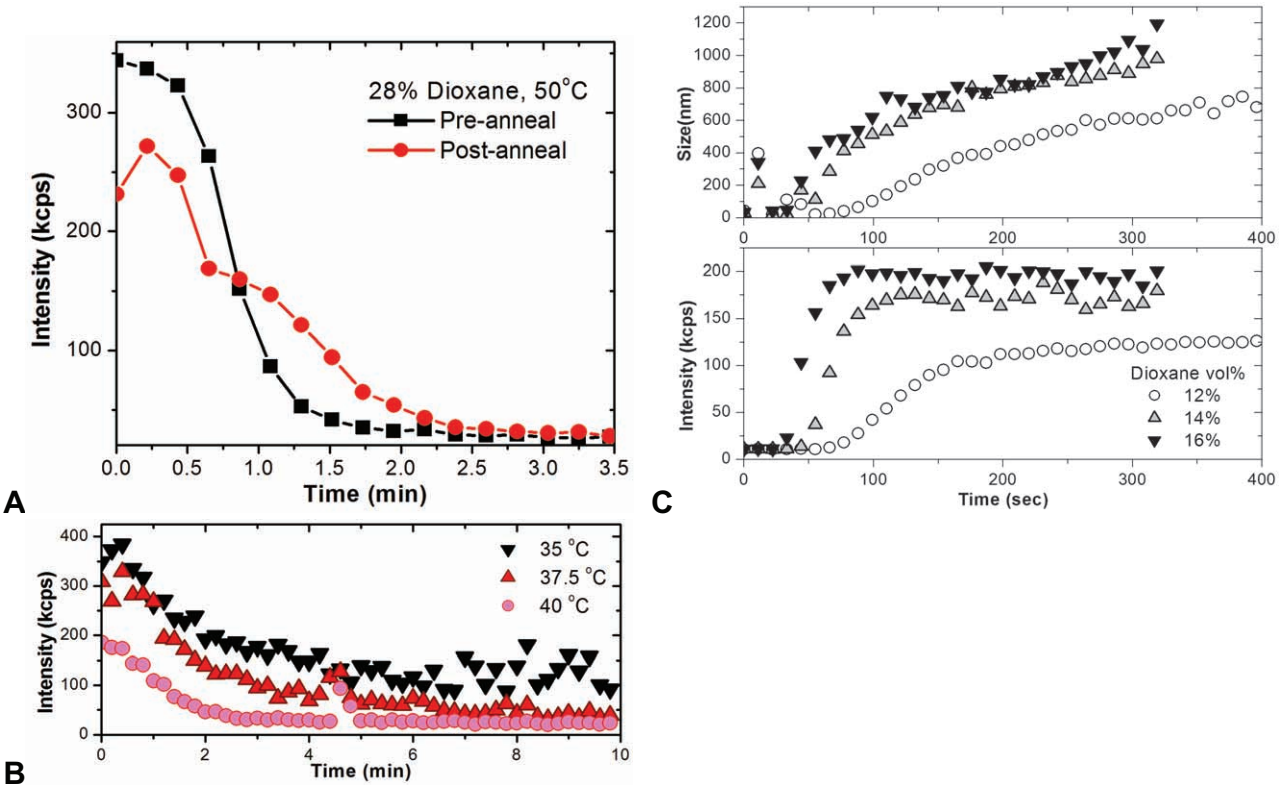

Figure S9. Scattering intensity and reported particle size by DLS of 0.2 μM nanorod solutions over time after immediate transfer from room temperature to a pre-heated or pre-cooled instrument. (A) Measurements of non-treated and heat treated nanorods in 28 vol% dioxane at 50 °C showing slower melting of the ordered assemblies. (B) Scattering intensity of assembled nanorods in 24 vol% dioxane heated to 35, 37.5, and 40 °C, very near the melting transition. (C) Aggregation curves for nanorods in 12, 14, and 16 vol% dioxane at 4 °C.

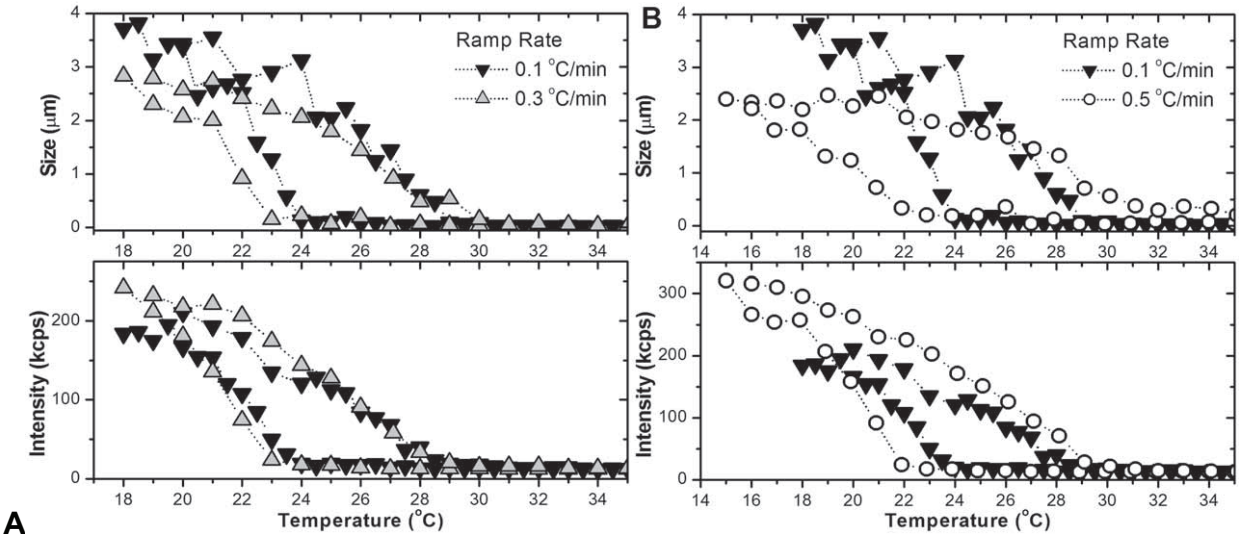

Figure S10. DLS data for 0.2 μM nanorods in 20 vol% dioxane heated and cooled (A) at 0.1 and 0.3 °C/min and (B) at 0.5 °C/min.

This journal is © The Royal Society of Chemistry 2012

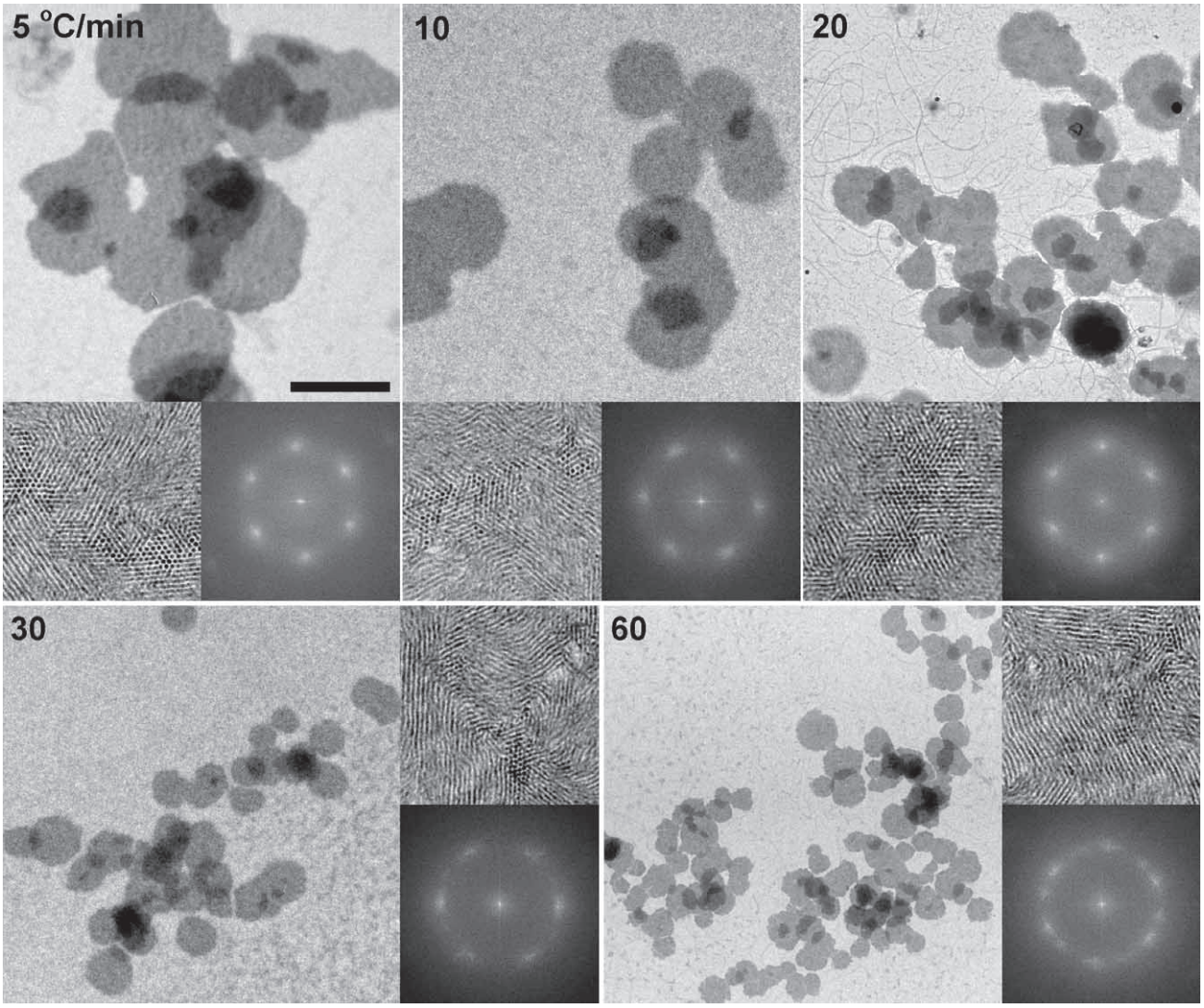

Figure S11. TEM images of 1.0 μM nanorod suspensions in 28 vol% dioxane heated to 60 °C and cooled at rates of 5-60 °C/min (12-1 sec/°C). Higher magnification images of 900 nm square areas were taken (cropped portions shown in insets), and FT analysis of the images show a deterioration of order with higher ramp rates. Scale bar is 3 μm and applies to all images except insets. Insets are 200 nm wide.

This journal is © The Royal Society of Chemistry 2012

7. Preliminary assembly of CdTe nanorods

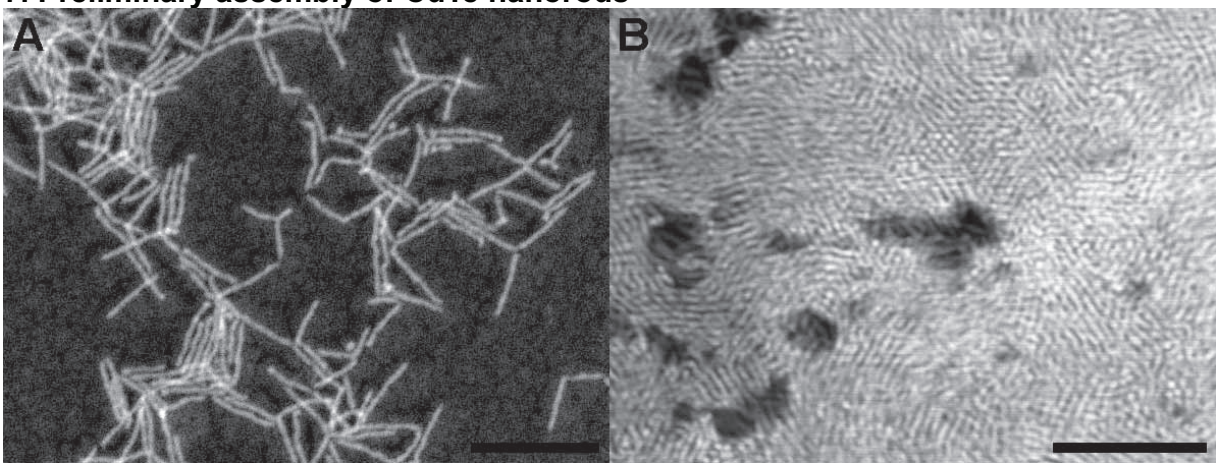

Figure S12. STEM images of a sample of CdTe nanorods and branched structures deposited (A) non-assembled from pure toluene and (B) assembled by thermal treatment in 28 vol% dioxane after cooling from 55 °C. The CdTe synthesis always yielded a greater population of branched structures which were expected to significantly reduce the degree of order in any assembled structure. However, a close-packed, layered film morphology was still observed despite the shape polydispersity, and small areas even showed some hexagonal packing. Scale bars are 100 nm.

8. References

[1] Z. A. Peng, X. G. Peng, J. Am. Chem. Soc. **124**, 3343 (2002).
[2] A. M. Hung, N. A. Konopliv, J. N. Cha, Langmuir **27**, 12322 (2011).
[3] J. L. Baker, A. Widmer-Cooper, M. F. Toney, P. L. Geissler, A. P. Alivisatos, Nano Letters **10**, 195 (2010).
[4] S. Ohe, *Vapor-Liquid Equilibrium Data* (Elsevier, New York, 1989).
[5] H. Holthoff, S. U. Egelhaaf, M. Borkovec, P. Schurtenberger, H. Sticher, Langmuir **12**, 5541 (1996).
[6] A. Zaccone, J. J. Crassous, B. Béri, M. Ballauff, Phys. Rev. Lett. **107**, 168303 (2011).